Optically switchable and tunable terahertz metamaterials through photoconductivity

2012 J. Opt. 14 114008

(http://iopscience.iop.org/2040-8986/14/11/114008)

J. Opt. **14** (2012) 114008 (8pp) doi:10.1088/2040-8978/14/11/114008

Optically switchable and tunable terahertz metamaterials through photoconductivity

M Kafesaki[1,2], N H Shen[3], S Tzortzakis[1,2] and C M Soukoulis[1,3]

[1] Institute of Electronic Structure and Laser, Foundation for Research and Technology Hellas (FORTH), PO Box 1385, 71110 Heraklion, Crete, Greece
[2] Department of Materials Science and Technology, University of Crete, 71003 Heraklion, Crete, Greece
[3] Ames Laboratory-USDOE, and Department of Physics and Astronomy, Iowa State University, Ames, IA 50011, USA

E-mail: kafesaki@iesl.forth.gr

Received 10 April 2012, accepted for publication 5 July 2012
Published 26 September 2012
Online at stacks.iop.org/JOpt/14/114008

Abstract
We present both theoretical and experimental cases for realizing optically switchable and tunable split-ring resonator (SRR) metamaterials operating in the THz regime. This is achieved by suitably placing photoconducting semiconductors in the various SRR designs. Exciting the semiconductor by an optical pump beam, the realization of single- and multi-band switching, blue-shift and red-shift tunability, and broad-band phase modulation are demonstrated.

Keywords: metamaterials, switchable systems, tunable systems, SRRs

(Some figures may appear in colour only in the online journal)

1. Introduction

The emerging technologies of THz sources along with the novel and unique potential applications of THz radiation [1], especially in imaging, security, and communication domains, make the need for THz manipulation components more and more imperative. Since the majority of natural materials do not show a strong response to THz radiation, and thus fail to offer easy handling and manipulation of the THz waves, metamaterials, i.e., artificially structured materials with subwavelength building blocks [2], seem to offer an excellent path towards this direction. The ability of metamaterials to strongly respond to THz radiation is due to the fact that by properly scaling the metamaterial building blocks, one can tune and adjust the metamaterial frequency regime of operation. Likewise, by properly designing the geometry of the metamaterial building blocks, one can control the type of operation and the metamaterial property achieved. Therefore, structures can be obtained with either high positive or negative permittivity values, high positive or negative permeability (even in the optical regime), negative index of refraction (leading to potential for subwavelength resolution imaging [3]), index close to zero (leading to possibility for cloaking [4] and beam collimation and steering [5]), etc.

Although the realization of passive metamaterial-based THz components, such as filters, polarizers, absorbers, etc, is of great importance for filling the 'THz gap', for the full manipulation and exploitation of THz waves, the achievement of active, dynamically controllable metamaterial elements is also essential, since it offers the possibility for the creation of a variety of active components, including tunable notch filters, switches, modulators, etc. With this target many efforts have been devoted to the realization of frequency agile metamaterial components, mainly in the THz [6–13] but also in the optical regime [14], in infrared [15, 16], and in microwaves [17–21]. Such metamaterials are realized by combining standard metamaterial elements with active materials, i.e., materials that can change optical properties by application of an external stimulus, such as voltage, light, temperature, mechanical stress, magnetic field, etc. The majority of the existing efforts on active metamaterial elements operating in THz concern metamaterials incorporating semiconductors, which

can change conducting properties by applying an external voltage or an external optical or UV light.

The basic metamaterial component used for the creation of active metamaterials is the split-ring resonator (SRR) structure [22], either in its original form, initially proposed by Pendry for the achievement of negative permeability (but capable also of giving negative permittivity, due to its bianisotropic response [23, 24]), or in more complicated forms [25] exhibiting multiple resonances, which, under excitation by a normally incident electromagnetic wave (i.e., excited by the incident electric field), result in most of the cases of resonant permittivity response of the total structure. Such resonators are usually described as effective capacitor–inductor circuits and the role of the semiconducting material, if incorporated in the resonator system, is either to short the circuit or to alter its capacitance (C) or inductance (L), thus modifying its resonance frequency, $\omega = 1/\sqrt{LC}$. Using such various shaped ring resonators, known also as electric-field coupled LC (ELC) resonators, various electrically tunable (i.e. tunable using an external voltage) metamaterials have been obtained, showing either blue-shift or red-shift tunability, or switching response [6, 7]. Moreover, a variety of optically controllable metamaterials have been realized, including blue- or red-shift tunable structures [8, 10], single and multi-band switches [9, 11], amplitude and/or phase modulators [12].

At present, control of optical metamaterials has been realized mainly by employing as 'active' materials photoconducting semiconductors, which, by the application of an external pump light, can be switched between insulating and conducting states to alter the metamaterial response. To incorporate such semiconducting materials into the metamaterial, two main approaches have been applied: (1) the semiconductor has been used as a metamaterial substrate or as a layer between the substrate and the metamaterial [9, 11, 12], and (2) the semiconductor is inserted locally into specific, critical parts of the metamaterial resonator [8, 10]. The first approach is easier in its practical implementation (in terms of fabrication), but it has the disadvantage that by application of the pump light, the total frequency spectrum of the metamaterial response is modified—not just selected frequency regimes close to the SRR resonances. This feature can be advantageous, depending on the desired property or application foreseen for the metamaterial. For example, in the case of double resonant metamaterials, one can exploit the frequency regime between the two resonances, where interesting phase modulation properties can be achieved. The second approach, i.e., the inclusion of the semiconductor into specific parts of the metamaterial resonator, although more difficult in its implementation, has the advantage of affecting specific frequency regions of the metamaterial response; therefore, leaving unaffected the remainder of the metamaterial spectrum.

In this brief review paper, we summarize our efforts to achieve optically controllable THz metamaterials [9, 10, 12] based on the incorporation of semiconductors into metamaterial elements and the employment of the above-mentioned approaches to incorporate the semiconducting material into the metamaterial. We demonstrated a variety of optically induced effects, including blue- and red-shift tunability of the metamaterial resonances, single- and multi-band switching, and broad-band phase modulation. Most of the above effects have been demonstrated theoretically (using full-wave simulations) and experimentally (employing THz time domain spectroscopy).

The remainder of this paper is organized as follows: section 2 briefly describes the numerical and experimental characterization procedures used to describe the optical response of our metamaterials. Section 3 presents the switchable and tunable metamaterial response capabilities achieved as a result of modulation of loop-current-based resonances of the metamaterial building blocks. Section 4 describes tunable and controllable metamaterials by modulation of dipole-like metamaterial resonances and off-resonance frequency regimes. Conclusions are presented in section 5.

2. Numerical and experimental characterization approaches

For the numerical characterization of our metamaterials, we used the finite integration technique employed through the Microwave Studio commercial software. For the calculation procedure, one unit cell of the metamaterial was placed inside a waveguide with the setting of periodic boundary conditions at its side-walls to support a constant profile transverse electromagnetic wave. Waveguide ports were placed at the entrance and exit of the waveguide, serving as source and detector, respectively, for the THz radiation perpendicularly incident on the sample.

To simulate the photoconducting semiconductor response, we used different values of conductivity to reflect the different levels of photoexcitation, as a result of different values of an applied pump power. In the case of resonance modulation based on loop currents, the change of the real part of the conductivity was sufficient to describe the experimentally observed resonance modulation. For modulation of dipole-like resonances or of non-resonant regimes, where the dielectric-like response of the environment plays a more critical role, the change of the imaginary part of the conductivity (or of the real part of the permittivity) according to the Drude model, was also taken into account.

For the experimental characterization of the samples, a powerful THz time domain spectroscopy (TDS) scheme was utilized. The THz radiation was generated through a non-linear process involving an amplified kHz Ti:Sa laser system delivering 35 fs pulses of central wavelength 800 nm and maximum energy 2.3 mJ/pulse. Using 1.3 mJ, part of the initial beam was focused in air after partial frequency doubling in a beta-barium-borate crystal to produce a two-color filament and, subsequently, THz radiation [10]. To detect THz radiation, the THz-induced birefringence in an electro-optic crystal (ZnTe) was probed by a small part of the initial laser pulse, monitoring the time profile of the THz electric field. The frequency profile of the electric field was obtained by Fourier transform of the time profile, while for the evaluation of the transmission amplitude through the

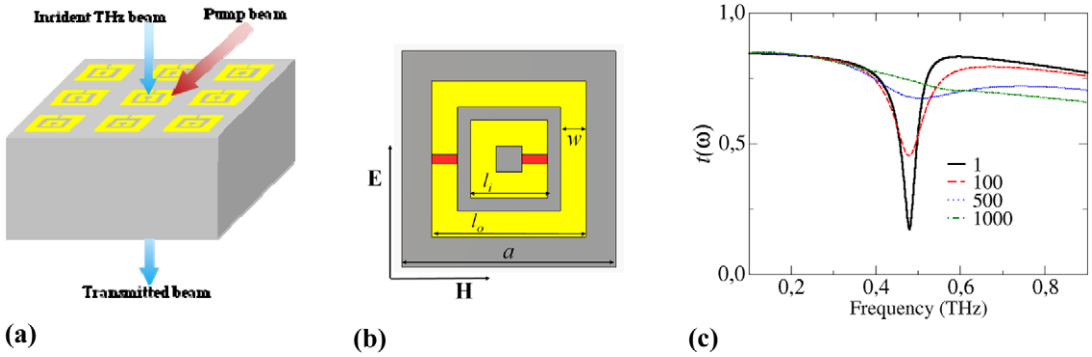

Figure 1. (a) The THz TDS pump–probe scheme employed for the experimental characterization of the structures under investigation. (b) The unit cell of an SRR system like the one studied in [9] and [10], but with photoconducting semiconductor (Si—see red color) only in the SRR gaps. The SRR parameters are unit cell linear size $a = 50$ μm, outer ring length $l_o = 36$ μm, inner ring length $l_i = 18$ μm, $w = 6$ μm, gap size 2 μm, and metal thickness 3 μm. (c) The transmission amplitude for a system of SRRs with a unit cell as shown in panel (b), for values of the conductivity for the photoconductive semiconductor as shown by the legends.

sample the transmitted field, $E(\omega)$, was divided by a reference system (usually the substrate alone).

To study the dynamic response of the metamaterial, the metamaterial was placed at the focus of the THz radiation at normal incidence, while an optical pump beam of wavelength 800 nm was used to excite photocarriers in the photoconducting semiconductor. The temporal delay between the optical pump beam and the THz beam was 5 ps, ensuring a quasi-steady-state for the charge carriers in the semiconductor (the life time for charge carriers is a few hundred nanoseconds). The application of the THz TDS scheme on our samples, along with the photoexcitation approach, is illustrated in figure 1(a).

3. Switching or tuning the loop-current-based resonances in simple and complex SRR structures

Since the resonant response of the SRR-based structures originates in most cases from the excitation of proper loop currents, which become resonant due to the presence of gaps in the metal (gaps act as capacitors, which impede the free current circulation and impose oscillations, and thus resonances), a simple and easy way to switch off this resonant response is to close the SRR gaps, shorting the effective SRR *LC* circuit. Such switching of the fundamental resonance (magnetic resonance) in conventional double-ring SRRs has been demonstrated by Padilla in a system of SRRs fabricated on top of a high resistivity GaAs substrate [11]. By illuminating the system using the pump optical beam, the excitation of photocurrents in the substrate shorted the SRR circuit, destroying the SRR resonance. As mentioned in the introduction and shown in figure 3(a) of [11], in this case, where the semiconductor is used as a substrate material, not only the resonance regimes but all the transmission spectrum of the metamaterial is affected by the change in the conducting properties of the semiconductor.

3.1. Single-band switch

A more efficient way to switch-off the SRR loop-current-based resonances without affecting the remainder of the spectrum is to place the photoconducting semiconductor only in the SRR gaps. In this case, the application of the pump beam excites photocurrents only at the gap regimes, which, in turn, short the SRR circuit, destroying the resonances but almost not affecting the remainder of the spectrum. In figure 1(b), we show the unit cell of a SRR metamaterial with geometrical features as in [11, 12] with the photoconducting material placed only at the SRR gaps. In figure 1(c), we show the calculated transmission spectrum for the system of figure 1(b), as the conductivity of the semiconductor increases from $\sigma = 1$ (corresponding to no optical pump power illumination) to $\sigma = 10^3$ S m^{-1} (corresponding to strong illumination). Here, the semiconductor is considered as Si, with permittivity 11.7 (and thickness 3 μm), while the SRR is made of copper, modeled as a lossy metal with conductivity 5.8×10^7 S m^{-1}. The SRR-Si system considered is placed on a sapphire substrate ($\varepsilon_{\text{sapphire}} = 10.5$).

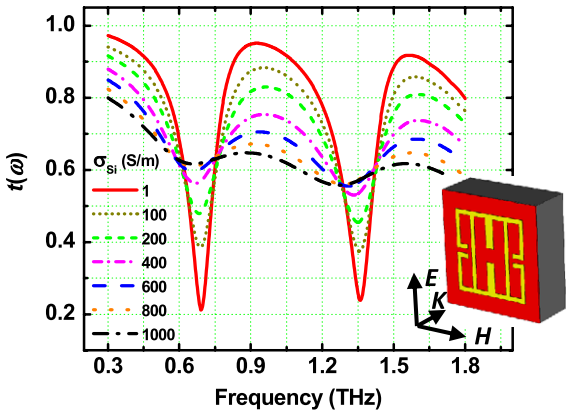

Figure 2. Simulated dual-band switching effect: transmission spectra as function of Si conductivity. The unit cell of the structure is shown in the inset; Si is marked with the red color.

3.2. Dual-band switch

Richer tuning and switching properties can be achieved if one employs SRRs of more complex shapes than the one shown in figure 1(b), with multiple loop-current resonances. Such an example is shown in the inset of figure 2, where a

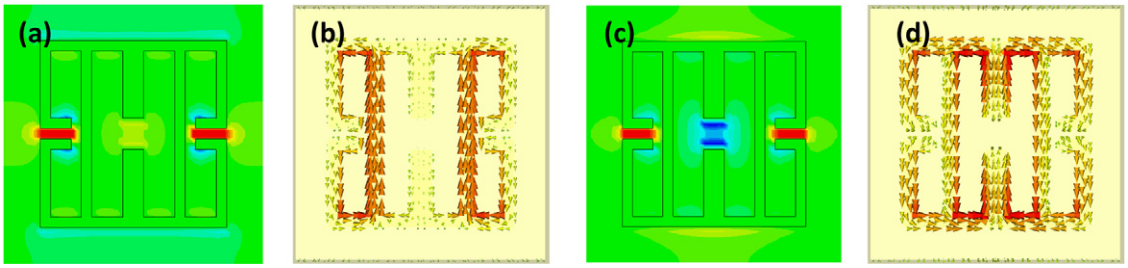

Figure 3. The electric field (a) and surface current distribution (b) at the lower frequency resonance of figure 2 (at 0.7 THz), and at the higher frequency resonance (electric field (c), and current (d)) at 1.38 THz.

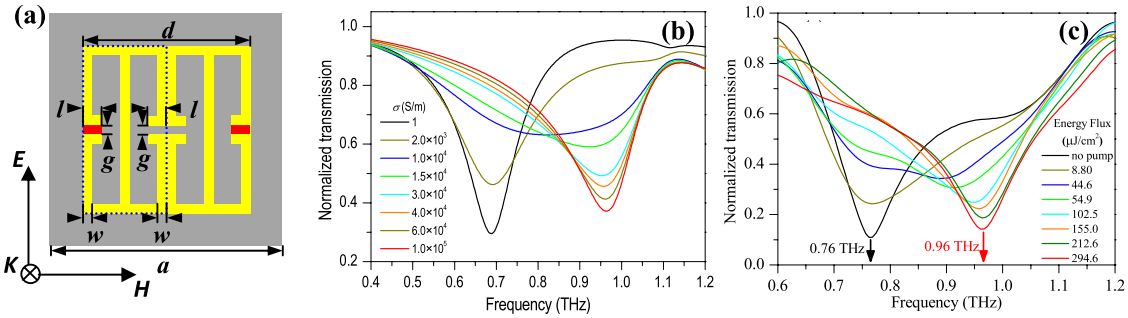

Figure 4. (a) The SRR design showing blue-shift tunability. The photoconducting material is shown with the red color. The geometrical features of the SRR are $a = 50\ \mu$m, $l = 4\ \mu$m, $d = 36\ \mu$m, $g = 2\ \mu$m, $w = 2\ \mu$m; the numerical transmission spectra through a system of such SRRs for different values of the conductivity of the photoconducting material (Si) placed at the outer SRR gaps (b), and the experimental transmission spectra for different intensities of the pumping source (c).

double resonance SRR is shown (yellow color) on top of a thin (600 nm) photoconducting (Si) layer (red color), placed on a sapphire substrate [9]. The simulated transmission through a system of such SRRs without pump power illumination is shown with the red-solid line in figure 2, revealing the presence of two distinct resonances—at 0.7 and 1.38 THz. The electric field and current distribution at these two resonances show that both originate from loop currents, see figure 3. The presence of the second resonance in the spectrum is based on the fact the capacitance of the central SRR gap is not equal to the capacitance of the side gaps; thus, the polarization induced in the central gap does not cancel that at the side gaps, resulting in non-zero average induced polarization.

As shown in figure 2, the pumping of the system of such SRRs by an optical pump beam results in the damping of both SRR resonances, due to the shorting of the circuits coming from the generation of photocurrents in the semiconductor. It also results in the reduction of transmission in the off-resonance frequency regimes, due to the increase of absorption in the semiconductor [9].

3.3. Blue-shift tunability in a system of SRRs

Another interesting SRR design is shown in figure 4(a) [9, 10], a symmetrized variation of the design shown in figure 2 in such a way as the capacitance of the central gap is equal to that of the two side gaps (this way only the first resonance of figure 2 can be excited by a normally incident EM wave).

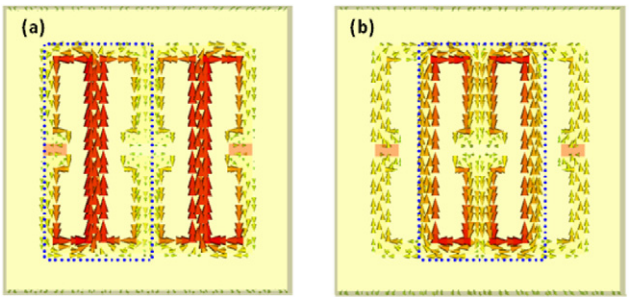

Figure 5. The distribution of the surface current at the first (a) and second (b) resonant modes shown in figure 4(b).

This SRR can be transformed to a blue-shift tunable structure by incorporating a photoconducting semiconductor, in our case Si, in the outer SRR gaps (as illustrated with the red color in figure 4(a)). The blue-shift tunable response of the system is demonstrated in figure 4(b), where the simulated transmission through the structure is shown for different values of Si conductivity, corresponding to different levels of pump power [10]. As shown in figure 4(b), by increasing the Si conductivity, the SRR resonance, while it initially weakens, beyond some conductivity values it reappears at higher frequencies, regaining strength and showing a blue-shift as high as 37%. This large blue-shift tunability, concluded by examining the field and current distributions in the cases with and without pumping (see figure 5), is a result of mode switching. By closing the outer SRR gaps, the system

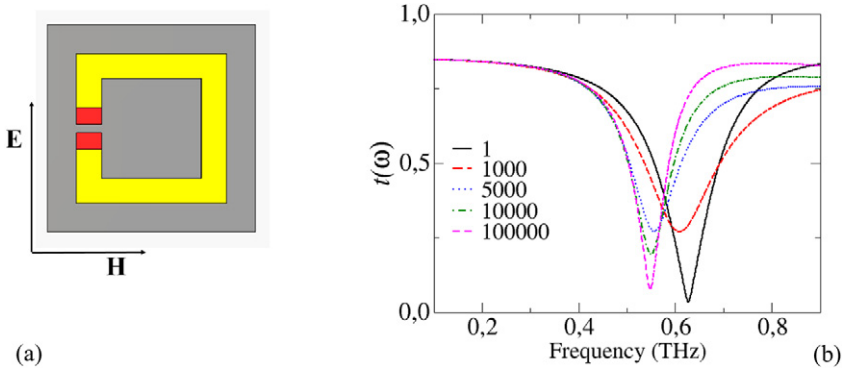

Figure 6. The SRR design showing red-shift tunability (a). The dimensions and the materials are the same as the unit cell and outer ring of figure 1(b), but the size of the semiconductor (red color) along the **E** direction is 5 μm at each side of the gap. Panel (b) shows the numerical transmission spectra through a system of SRRs such as the one in panel (a) for different values of the conductivity of the photoconducting semiconductor (Si). Legends show the Si conductivity in S m^{-1}.

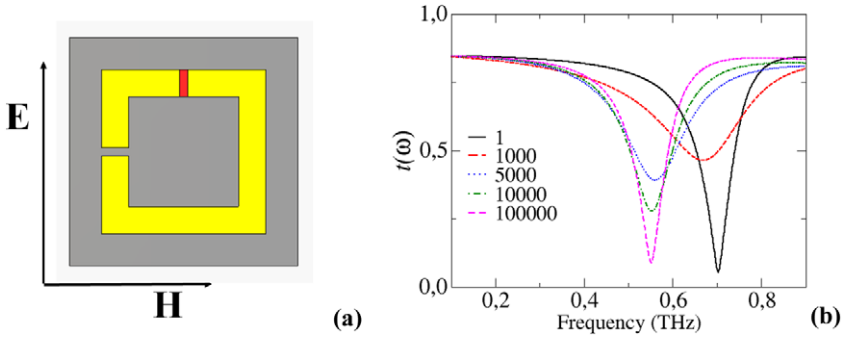

Figure 7. A two-gap single-ring SRR design showing red-shift tunability (a). The materials and dimensions are the same as the SRR of figure 1(b), with the inner ring missing. The gap size is 2 μm for both gaps—one is filled with Si (red color). Panel (b) shows the numerical transmission spectra through a system of such SRRs for different values of the conductivity (mentioned in the legends—in S m^{-1}) of the photoconducting Si.

switches between a lower frequency mode, with resonance at ∼0.7 THz, and a higher frequency mode, with resonance at ∼0.96 THz. The current distribution associated with these two modes is shown in figure 5.

The SRR system of figure 4(a) has been fabricated and characterized experimentally [10]. The fabrication of the metallic parts was achieved by UV lithography and the Si (of thickness 2 μm) was deposited using reactive ion etching (for the fabrication details see [10]). The experimental transmission data, obtained through the THz time domain spectroscopy scheme described in section 2, are shown in figure 4(c) for different pump power levels, and are in quite good agreement with the corresponding numerical results (figure 4(b)).

3.4. Red-shift tunability in a system of SRRs

The achievement of red-shift tunability in SRR systems is quite easier than achievement of blue-shift tunability, as it is sufficient to incorporate the photoconducting semiconductor into the design in such a way as to increase the SRR capacitance upon illumination with the pumping beam. An easy method to increase this capacitance is to partially cover the gaps of even simple SRR designs by the photoconducting semiconductor [17], shown in figure 6(a). The pumping of a system of SRRs such as the one in figure 6(a) by an optical beam results in the transmission spectrum shown in figure 6(b), demonstrating red-shift tunability. The degree of tunability in this case strongly depends on the size of the gap and the percentage of the gap covered by the photoconducting semiconductor.

Another easy approach with the potential to offer a larger degree of red-shift tunability than the approach of figure 6 is to employ a multigap SRR structure (mirror-asymmetric in respect to the applied electric field), shown in figure 7(a), and fill one of its gaps with the photoconducting semiconductor (preserving though the mirror asymmetry of the structure). Then, the pump power illumination will sort the 'capacitor' covered with the semiconductor, increasing the total capacitance of the structure (in a single-ring multigap SRR, the gaps can be considered as capacitors connected in series). The transmission through a system of SRRs, such as the one in figure 7(a), for different values for the conductivity of the photoconducting semiconductor (Si) corresponding to different pump power intensities, is shown in figure 7(b), showing a tunability as high as ∼30%.

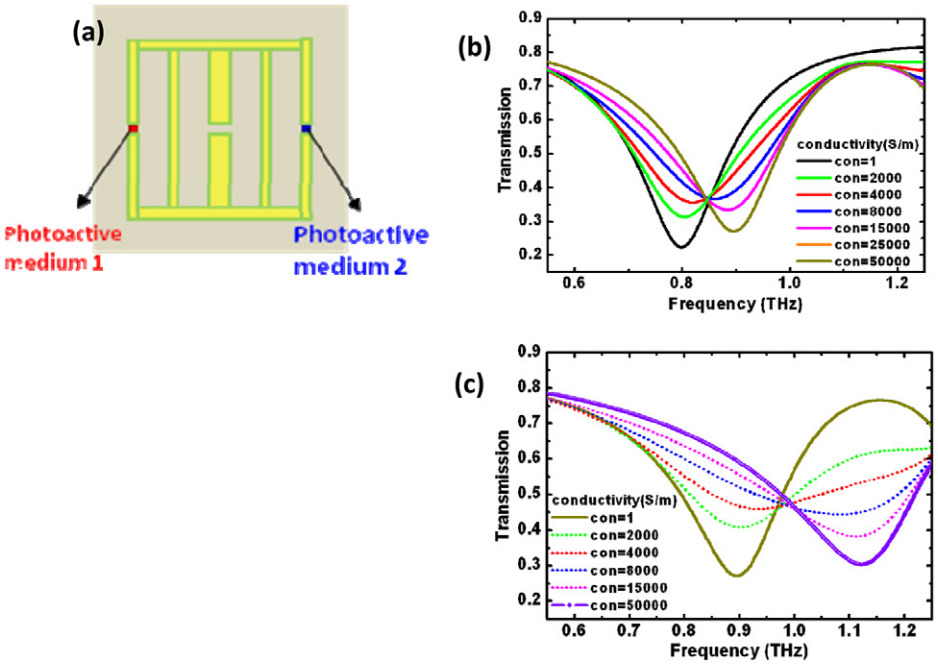

Figure 8. (a) The SRR design showing multi-mode switching. The geometrical parameters of the design are the same as in the one in figure 4. Numerical transmission spectra through a system of such SRRs for excitation of the photoconducting medium 1 (conductivity here refers to medium 1) (panel (b)), and medium 2, with medium 1 fully excited. Conductivity here refers to medium 2, while the conductivity of medium 1 has been taken as 50 000 S m^{-1} (panel (c)).

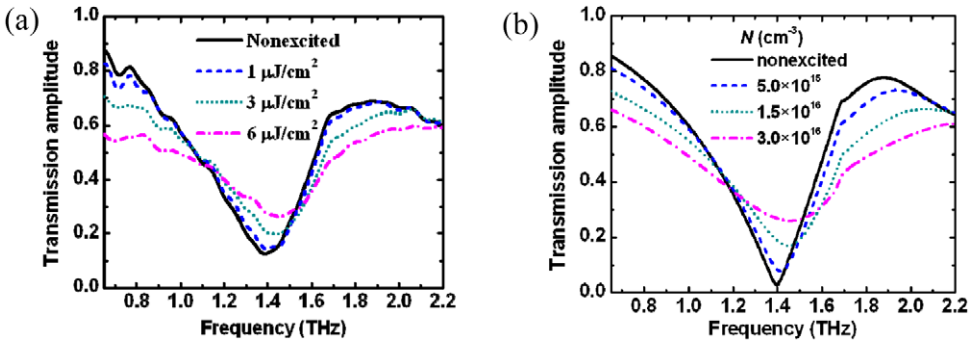

Figure 9. Experimental (a) and simulated (b) transmission amplitude spectra for different levels of photoexcitation of a system of SRRs (with geometrical features as described in figure 1(b)) on top of a GaAs substrate.

3.5. Multi-mode switching in SRR systems

A very useful component for THz handling and manipulation is a multi-mode switch. Such a switch can be achieved by employing a multigap SRR design, similar to the one in figure 4, and depositing at its two outer gaps two different semiconductors (i.e., with different bandgap energies), which can be excited using two different pumping sources. Figure 8(a) shows the design of such an example. Figure 8(b) shows the transmission under illumination with a laser exciting one of the two semiconductors (photoactive medium 1) and figure 8(c) demonstrates the transmission under illumination with a laser exciting also the second semiconductor. One can see in figure 8 that the design can operate as a three-mode switch with all modes having almost the same strength.

4. Blue-shift tunability and broad-band phase modulation in traditional SRR structures away from the loop-current resonance

For the achievement of active THz metamaterials, one can benefit not only from loop-current-based resonances but also from higher-order resonances, such as dipole resonances of the SRRs or off-resonance frequency regimes. Employing conventional (Pendry) SRRs, like the one in figure 1, fabricated on top of GaAs substrate [12], the excitation of photocarriers in the substrate results in a blue-shift of the dipole-like resonance, as demonstrated by the experimental data presented in figure 9 [12]. We note here that for the results of figure 9, the SRRs are oriented so as to provide mirror symmetry in respect to the applied THz electric field; in this case, the lowest frequency resonance that can be excited by the electric field is the dipole-like resonance. To understand

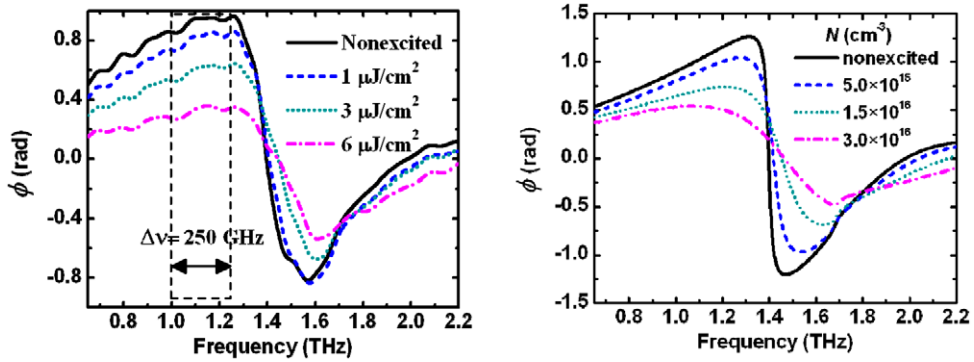

Figure 10. Experimental (a) and simulated (b) phase tunability for different levels of photoexcitation for the same SRR system as in figure 9.

and reproduce theoretically the blue-shift of this resonance, it is essential to take into account the photoexcitation induced change not only to the real part of the substrate conductivity, but also to the imaginary part, i.e., to the real part of the substrate permittivity representing the change in the dielectric properties of the substrate. According to the Drude model, $\varepsilon = \varepsilon_{\mathrm{GaAs}} - \omega_{\mathrm{p}}^2/(\omega^2 + \mathrm{i}\omega\gamma)$, with $\omega_{\mathrm{p}} = \sqrt{Ne^2/\varepsilon_0 m^*}$, $m^* = 0.067m$, $\gamma = 1.8$ THz, $\varepsilon_{\mathrm{GaAs}} = 12.7$, where ω_{p} is the semiconductor plasma frequency, γ its collision frequency, and m^* the effective mass of the carriers, an increase of the carriers density (N) due to photoexcitation results in a reduction of the substrate permittivity and, therefore, in the blue-shift of the dipole-like SRR resonance frequency. To reproduce numerically (see figure 9(b)) the experimentally obtained transmission, we considered carrier densities 3×10^{16}, 1.5×10^{16}, 5×10^{15} cm^{-3} for excitations 6, 3, and 1 μJ cm^{-2}, respectively, and penetration depth for the optical pump beam as 1 μm.

Another interesting feature observed in the system described in connection with figure 9 concerns the phase modulation at frequencies below the resonance as we increase the optical pumping intensity. Figure 10, which shows the phase of the transmitted wave (obtained both theoretically and experimentally) for various values of the pumping intensity, demonstrates a broad-band (∼250 GHz) phase modulation in the frequency regime below the resonance, associated with almost no change in transmitted intensity. This large (over $\sim\pi/4$) phase modulation demonstrates the potential for our metamaterial to be used as a tunable THz wave plate.

5. Conclusions

In this paper we reviewed our studies on optically tunable and switchable THz metamaterials. The metamaterials are based on electrically resonant SRR structures of various designs, suitably incorporating photoconducting semiconductors, which, under excitation by an optical pump beam, can change from an insulating to a conducting state, modulating the metamaterial response. The semiconductors are either employed as substrate materials or are placed in critical parts of the SRR structure. This approach, exploiting loop-current resonances of the SRRs, demonstrated single- and multi-band switchable structures, tunable SRRs showing either blue- or red-shift tunability, and multi-mode SRR switches. Moreover, exploiting dipole-like SRR resonances demonstrated blue-shift tunability and a broad-band phase modulator. The switchable/tunable SRR structures demonstrated here can form the basis for a variety of THz manipulation components, such as tunable notch filters, switches, and tunable wave-plates, offering additional solutions to fill the 'THz gap.'

Acknowledgments

We acknowledge financial support by the EU projects PHOME, NIMNIL and ENSEMBLE, and by the COST Action MP0803. Work at Ames Laboratory was supported by the Department of Energy (Basic Energy Sciences, Division of Materials Sciences and Engineering) under Contract No. DEAC02-07CH11358.

References

[1] Tonouchi M 2007 Cutting-edge terahertz technology *Nature Photon.* **1** 97
[2] Sihvola A 2007 Metamaterials in electromagnetic *Metamaterials* **1** 2
[3] Pendry J B 2000 Negative refraction makes a perfect lens *Phys. Rev. Lett.* **85** 3966
[4] Pendry J B, Schurig D and Smith D R 2006 Controlling electromagnetic fields *Science* **312** 1780
[5] Ziolkowski R W 2004 Propagation and scattering from a matched metamaterial having a zero index of refraction *Phys. Rev.* E **70** 046608
[6] Chen H-T, Padilla W J, Cich M J, Azad A K, Averitt R D and Taylor A J 2009 A metamaterial solid-state terahertz phase modulator *Nature Photon.* **3** 148
[7] Chen H-T, Padilla W J, Zide J M O, Gossard A C, Taylor A J and Averitt R D 2006 Active terahertz metamaterial devices *Nature* **444** 597
[8] Chen H-T, O'Hara J F, Azad A K, Taylor A J, Averitt R D, Shrekenhamer D B and Padilla W J 2008 Experimental demonstration of frequency-agile terahertz metamaterials *Nature Photon.* **2** 295
[9] Shen N-H, Kafesaki M, Koschny Th, Zhang L, Economou E N and Soukoulis C M 2009 Broadband blueshift tunable metamaterials and dual-band switches *Phys. Rev.* B **79** 161102
[10] Shen N-H, Massaouti M, Gokkavas M, Manceau J-M, Ozbay E, Kafesaki M, Koschny Th, Tzortzakis S and Soukoulis C M 2011 Optically implemented broadband

blueshift switch in the terahertz regime *Phys. Rev. Lett.* **106** 037403
[11] Padilla W J, Taylor A J, Highstrete C, Lee M and Averitt R D 2006 Dynamical electric and magnetic metamaterial response at terahertz frequencies *Phys. Rev. Lett.* **96** 107401
[12] Manceau J-M, Shen N-H, Kafesaki M, Soukoulis C M and Tzortzakis S 2010 Dynamic response of metamaterials in the terahertz regime: blueshift tunability and broadband phase modulation *Appl. Phys. Lett.* **96** 021111
[13] Driscoll T, Kim H-T, Chae B-G, Kim B-J, Lee Y-W, Jokerst N M, Palit S, Smith D R, Di Ventra M and Basov D N 2009 Memory metamaterials *Science* **325** 1518
[14] Wang X, Kwon D-H, Werner D H, Khoo I-Ch, Kildishev A V and Shalaev V M 2007 Tunable optical negative-index metamaterials employing anisotropic liquid crystals *Appl. Phys. Lett.* **91** 143122
[15] Werner D H, Kwon D-H, Khoo I-Ch, Kildishev A V and Shalaev V M 2007 Liquid crystal clad near-infrared metamaterials with tunable negative-zero-positive refractive indices *Opt. Express* **15** 3342
[16] Driscoll T *et al* 2008 Dynamic tuning of an infrared hybrid-metamaterial resonance using vanadium dioxide *Appl. Phys. Lett.* **93** 024101
[17] Degiron A, Mock J J and Smith D R 2007 Modulating and tuning the response of metamaterials at the unit cell level *Opt. Express* **15** 1115
[18] Hand Th H and Cummer S A 2008 Frequency tunable electromagnetic metamaterial using ferroelectric loaded split rings *J. Appl. Phys.* **103** 066105
[19] He Y, Yoon P S D, Parimi P V, Rachford F J, Harris V G and Vittoria C 2007 Tunable negative index metamaterial using yttrium iron garnet *J. Magn. Magn. Mater.* **313** 187
[20] Shadrivov I V, Morrison S K and Kivshar Y S 2006 Tunable split-ring resonators for nonlinear negative-index metamaterials *Opt. Express* **14** 9344
[21] Vendik O G and Zubko S P 2009 Ferroelectrics as constituents of tunable metamaterials *Theory and Phenomena of Metamaterials* ed F Capolino (Boca Raton, FL: CRC Press)
[22] Pendry J B, Holden A J, Robbins D J and Stewart W J 1999 Magnetism from conductors and enhanced nonlinear phenomena *IEEE Trans. Microwave Theory Technol.* **47** 2075
[23] Marques R, Medina F and Rafii-El-Idrissi R 2002 Role of bianisotropy in negative permeability and left-handed metamaterials *Phys. Rev.* B **65** 144440
[24] Katsarakis N, Koschny T, Kafesaki M, Economou E N and Soukoulis C M 2004 Electric coupling to the magnetic resonance of split ring resonators *Appl. Phys. Lett.* **84** 2943
[25] Padilla W J, Aronsson M T, Highstrete C, Lee M, Taylor A J and Averitt R D 2007 Electrically resonant terahertz metamaterials: theoretical and experimental investigations *Phys. Rev.* B **75** 041102(R)